

Article

# Spatiotemporal Variations in Seston C: N: P Stoichiometry in a Large Eutrophic Floodplain Lake (Lake Taihu): Do the Sources of Seston Explain Stoichiometric Flexibility?

Jian Cai<sup>1</sup>, Chengrong Bai<sup>2</sup>, Xiangming Tang<sup>1</sup>, Jiangyu Dai<sup>3</sup>, Xingyu Jiang<sup>1,2</sup>, Yang Hu<sup>1</sup>, Keqiang Shao<sup>1</sup> and Guang Gao<sup>1,\*</sup>

<sup>1</sup> State Key Laboratory of Lake Science and Environment, Nanjing Institute of Geography and Limnology, Chinese Academy of Sciences, Nanjing 210008, P. R. China

<sup>2</sup> University of Chinese Academy of Sciences, Beijing, 100049, P. R. China

<sup>3</sup> State Key Laboratory of Hydrology-Water Resources and Hydraulic Engineering, Nanjing Hydraulic Research Institute, Nanjing, 210029, P. R. China

\* Correspondence: guanggao@niglas.ac.cn; Tel. (+86) 25 86882213; Fax (+86) 25 57714759

**Abstract:** Although sources of seston are much more complicated in lakes compared to marines, the influences of different source on the spatiotemporal variations in seston stoichiometry are still underexplored, especially in large eutrophic floodplain lakes. Here, we investigated the seston stoichiometry across a typical large eutrophic floodplain lake (Lake Taihu) over one year. In addition, we used the *n*-alkanes proxies for source estimation which are more robust than other elemental indicators (e.g. C: N ratios). Throughout the study, the average value of C: N: P ratio of 143: 19: 1 across Lake Taihu was higher than the classical Redfield ratio, but closed to the synthesized data from other lakes. Generally, seston C: N ratios varied the least across all environments, but C: P and N: P ratios varied widely and shown a significant seasonal pattern with lower ratios of N: P and C: P during senescence seasons and higher ratios in the growing seasons. This seasonal change was mainly associated with the shift from terrestrial-derived seston to algal-derived seston as, the significant lower ratios of terrestrial-derived seston from surrounding agricultural watershed. Spatially, the mean ratios of each site were similar, except relative higher values of C: P and N: P ratios in the algal dominated area. Statistically, the predictive power of environmental variables on stoichiometric ratios was strongly improved by adding *n*-alkanes proxies. Apart from sources indicators, particulate phosphorus (PP) contents also partly explained the spatiotemporal variations in stoichiometric ratios. Nevertheless, the mechanisms behind the dynamics of PP could be totally different and source-specific. This study highlights the priority of using *n*-alkanes proxies as tools to identify the source of seston which is essential to interpret the spatiotemporal variations in seston stoichiometric ratios among eutrophic floodplain lakes.

**Keywords:** seston stoichiometry; source estimation; *n*-alkanes proxies; large eutrophic floodplain lakes; Lake Taihu

## 1. Introduction

The C: N: P ratio of suspended particulate matters, hereafter “seston”, is closely tied to biogeochemical cycles and food webs in aquatic ecosystems [1–3]. Since A. C. Redfield first observed that C: N: P ratios of seston in the offshore surface ocean are similar to the ratios of dissolved nutrients in the deep ocean, the Redfield ratio (e.g., the canonical Redfield ratio of C: N: P = 106:16:1) is routinely used to interpret and predict ecosystem processes in oceans [4]. While increasing evidence has shown that C: N: P ratios can vary at spatial and temporal scales, the general applicability of the canonical

Redfield ratio is under debated [5]. In marine ecosystems, seston often exhibits small deviations from the Redfield ratio and follows some general patterns, for example associating with latitudinal gradient, seasonal cycles and depth profiles [6–8]. In contrast, among lakes, seston shows higher ratios (C:N:P = 166:20:1) and more than 10-fold variations [9]. In order to introduce seston stoichiometry into lake ecological studies, the causes of its great spatial and temporal variability in lakes are of considerable interest.

In the majority of studies to date, a long list of various biotic and abiotic causes have been advocated for the flexible seston C: N: P ratios, including taxonomic composition of phytoplankton, nutrient availability, temperature, light intensity and seston mass, which drive the variability of seston stoichiometry through directly or indirectly affecting elemental ratios of algal cells [6,7,9–11]. However, when taking these factors into account, it is of vital importance to consider the source of seston in advance. As if the seston is mainly comprising of allochthonous components, the responses of phytoplankton could be masked. The influence of allochthonous detritus to deviations of seston C: N: P ratios had been confirmed among temperate oligotrophic lakes [12]. However, the consideration of the seston sources is still scarce among eutrophic lakes. Although there is evidence proposed that the seston is dominated by algal biomass in eutrophic lakes, whereas most of these lakes are characterized long water residence time and few riverine inputs [13,14]. In fact, the contribution of terrestrial matters is unignorable in many eutrophic floodplain lakes, where river-lake interactions are intensive [15]. Moreover, as short residence times of floodplain lakes, the high input of terrestrial components tends to dominate the seston pool when algal blooming is fading away [16,17]. Last but not least, many large floodplain eutrophic lakes are also partly covered by macrophytes (Zhang et al., 2017). Therefore, the influence of different sources on variations in seston stoichiometry has to be reconsidered in large eutrophic floodplain lakes.

Lake Taihu, similar to other large eutrophic floodplain lakes, is often characterized as serious cyanobacterial blooms, intensive riverine inputs and great spatial [19]. Due to its high-level eutrophication, the cyanobacterial blooms are prevailing during the growing seasons (from late spring to early autumn), and fading away during senescence seasons (from late autumn to early spring) [20]. Meanwhile, the majority of riverine input enters the lake mostly via tributaries which bring higher eutrophic stress and larger amounts of allochthonous particles in the vicinity of inlets and adjacent lakeshores, than further away [21]. Lake Taihu's shallowness means that there is frequent mixing process, which can change within lake heterogeneity. These topographic and environmental characteristics likely cause significant variation in seston C: N: P ratios. But, compared to extensive investigations of dissolved and total nutrients in Lake Taihu, the particulate nutrients were poorly documented. The most comprehensive investigation of seston in Lake Taihu to date could be found in Shi (2018). However, they used C: N ratios as a source indicator of which reliability was under debated [22].

In this study, the seston C, N and P concentrations were monthly measured across Lake Taihu over one year, where the environmental data were simultaneously documented. In addition, *n*-alkane proxies were applied to identify the source of seston in Lake Taihu. Our primary objective was to characterize spatiotemporal variations in seston C: N: P stoichiometry in Lake Taihu and to relate this variation to other environmental factors, especially in terms of detailed attention to sources of seston. We further predicted that the temporal patterns in stoichiometric ratios would differ between each area where the main source of seston should be different.

## 2. Materials and Methods

### 2.1. Study sites

Samples were collected at five sites (Figure 1) that could be taken as representatives as four main sub-ecotypes of Lake Taihu [23]. Station DPE and ZSB are respectively situated on the estuary area of Dapu river and Yicun river, which are the two greatest inflow river of Lake Taihu [19]. Site MLB is located in Meiliang Bay, a region where cyanobacteria bloom is serious and riverine inputs are rigorously constrained. Station LC is located in the center of open lake, where the water is less

enriched with nutrients but exposed to more frequent wind-induced sediment resuspension. Sites XKB is located in Xukou Bay, a typical macrophyte zone near the outflow Xu river.

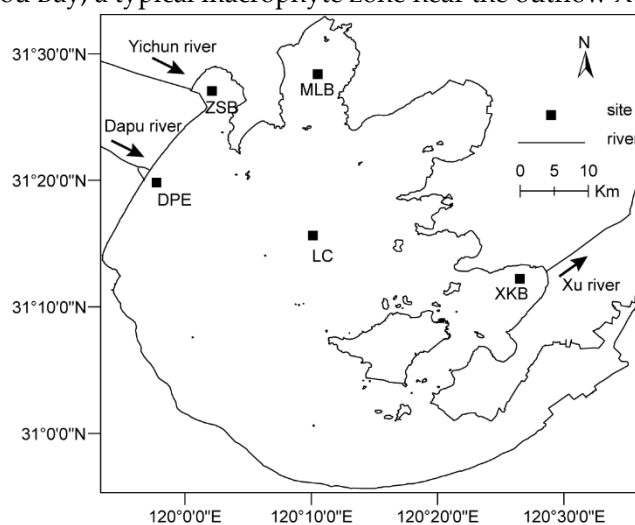


**Figure 1.** The map of Lake Taihu and sampling sites as illustrated.

## 2.2. Fieldworks

Monthly sampling works were carried out between June 2016 and May 2017. Five liters of sub-surface (0.5 m) water was collected from each site using an acid-cleaned plastic sampler. Due to the shallowness (e.g. mean depth is 1.9 m) and intensive wave-induced vertical mixing, the samples from sub-surface could represent the entire water column [24]. The water temperature (T) was measured in situ using YSI-6600 handle multiparameter meter (Yellow Springs Instruments, United States). All water samples were transferred in acid-washed 5L bottles and temporally stored at 4 °C before further analysis.

## 2.3. Sample processing and analyses

Using standard methods (Clescerl et al. 1999), total suspended solids (TSS) and chlorophyll *a* (Chl *a*) were quantified immediately upon return to the Taihu Laboratory for Lake Ecosystem Research (TLLER, <http://taihu.niglas.cas.cn/>). Water samples for dissolved nutrients were filtered through pre-ashed 0.7 µm glass fiber filters (GF/F, Whatman, United States), and all GF/F filters for seston stoichiometry and *n*-alkanes were freeze-dried and stored at -20 °C. The total dissolved phosphorus (TDP), the dissolved nitrogen (TDN), ammonium (NH<sub>4</sub><sup>+</sup>), and phosphate (PO<sub>4</sub><sup>3-</sup>) concentrations in filtrates were measured according to the standard analytical methods (Clescerl et al. 1999). The dissolved organic carbon (DOC) were determined on a TOC analyzer (Shimadzu, Japan). For analyzing the particulate organic carbon (POC) and particulate nitrogen (PN) in seston, frozen filters were thawed and dried at 50 °C for 1 h, then weighed and kept at room temperature in a desiccator. In order to remove carbonate fraction, these filters were fumed with HCl and re-dried in a clean fume hood. The carbon and nitrogen contents were subsequently determined on an NA-1500 elemental analyzer (Fisons Instruments, United States). The particulate phosphorus (PP) was analyzed on corresponding filters placed in 15 ml distilled water that acidified with H<sub>2</sub>SO<sub>4</sub> and digested with peroxodisulphate at 121 for 1 h [12]. The final phosphate concentration in digested solutions was measured spectrophotometrically as the same protocol as TP and TDP. The POC, PN and PP indicated the mass concentration per unit mass of TSS. The qPOC, qPN and qPP indicated the mass concentration per unit volume.

As shown in the previous study [25], the *n*-alkanes were extracted by the microwave method. Briefly, total lipids were first extracted from freeze-dried filters or biogenic materials with organic solvents (dichloromethane: methanol = 9: 1, v/v), using microwave bath. In order to remove alkenoates, the extracted solution was hydrolyzed within 6% KOH, and then neutral lipids were extracted with *n*-hexane. The *n*-alkane fraction was separated and collected from neutral lipids using

silica gel column chromatography. The concentrations of *n*-alkanes were quantified on an Agilent 7890 gas chromatography (Agilent Technologies, United States) with a flame ionized detector. The *n*-C<sub>36</sub> alkane was used as lab standards for peak identification and quantification.

#### 2.4. Calculation of *n*-alkane proxies

Several classical proxies of *n*-alkanes had been calculated to estimate the origins of seston, including the odd-to-even carbon preference index (CPI) [26], the ratio of long-chain to short-chain *n*-alkanes (L/H) [27], the ratio of terrigenous to aquatic odd *n*-alkanes (TARHC) [28], the ratio that reflects the non-emergent aquatic macrophyte to emergent aquatic and terrestrial plants (P<sub>aq</sub>) [29], and the modified *n*-alkane average chain length (ACL) between C16 and C32 [30]. These proxies were calculated as following equations:

$$\text{CPI} = \frac{1}{2} \times \left[ \left( \frac{\text{C}_{25} + \text{C}_{27} + \text{C}_{29} + \text{C}_{31} + \text{C}_{33}}{\text{C}_{24} + \text{C}_{26} + \text{C}_{28} + \text{C}_{30} + \text{C}_{32}} \right) + \left( \frac{\text{C}_{25} + \text{C}_{27} + \text{C}_{29} + \text{C}_{31} + \text{C}_{33}}{\text{C}_{26} + \text{C}_{28} + \text{C}_{30} + \text{C}_{32} + \text{C}_{34}} \right) \right] \quad (1)$$

$$\text{L/H} = \frac{\sum(\text{C}_{15-31})}{\sum(\text{C}_{22-33})} \quad (2)$$

$$\text{TARHC} = \frac{(\text{C}_{27} + \text{C}_{29} + \text{C}_{31})}{(\text{C}_{15} + \text{C}_{17} + \text{C}_{19})} \quad (3)$$

$$\text{P}_{\text{aq}} = \frac{(\text{C}_{23} + \text{C}_{25})}{(\text{C}_{23} + \text{C}_{25} + \text{C}_{29} + \text{C}_{31})} \quad (4)$$

$$\text{ACL} = \frac{\sum \text{C}_i \times i}{\sum \text{C}_i} \quad (5)$$

#### 2.5. Statistical analysis

General spatial differences in each seston stoichiometric ratio across sub-ecotypes and seasons were compared using the Kruskal-Wallis non-parametric test. Duncan tests were applied as post hoc multiple comparisons for differences among each site. Basing on previous studies [14,31], the four regular seasons were categorized into two periods: the growing seasons (from May to September) and senescence seasons (from October to April). Temporal differences in overall Lake and each site were compared using t-tests. Principle component analysis (PCA) was performed to investigate the genera pattern and association of *n*-alkane proxies and select the most representative proxies for further analysis.

Partial least squares regression (PLSR) was used in order to examine the relative influence (predictive power) of individual environmental variables on each stoichiometric ratio. Compared to ordinary linear regression, PLSR is more powerful to confront possibly correlating and non-normal predictors [32]. The relative influence of each variable was quantified using variable importance in the projection (VIP) scores where variables > 1.0 have strong influences, variables < 0.8 have weak influence, and variables in the middle range (0.8-1.0) have moderately influence [33,34].

### 3. Results

#### 3.1. Spatio-temporal variations in seston C: N: P stoichiometry

The seston C: N: P ratios were flexible with mean value (C: N: P = 143: 19: 1) across Lake Taihu being higher than expected by the canonical Redfield ratio of C: N: P = 106:16:1 (Figure 2). Seston N: P and C: P ratios ranged widely with the coefficient of variation (CV) of 44% and 40% respectively, whereas C: N ratios varied the least (CV=11%) throughout this investigation. Although the lowest C: N ratios could be observed in MLB (mean= 7.4), the values did not differ significantly between different locations. In contrast, the mean N: P and C: P ratios differed systematically across Lake Taihu. Both C: P and N: P ratios were highest at MLB (means=178.5 and 27.4, respectively), and

generally lower at estuary sites. The mean seston stoichiometric ratios were not significantly different between LC and XKB.

Regardless of spatial heterogeneity in Lake Taihu, strong effects of season on N: P and C: P ratios were shown as significantly higher values in growing seasons than senescence seasons (Figure 3b,c). Synchronously, seston C: P and N: P ratios in DPE, ZSB and LC significantly decreased after growing seasons. Seston C: P and N: P ratios in MLB also showed similar decreasing tendencies but not statistically significant. In contrast, although mean seston C: N ratios in DPE increased significantly from senescence seasons to growing seasons, while this difference of C: N ratios were not significant within other sites or entire lake datasets (Figure 3a).

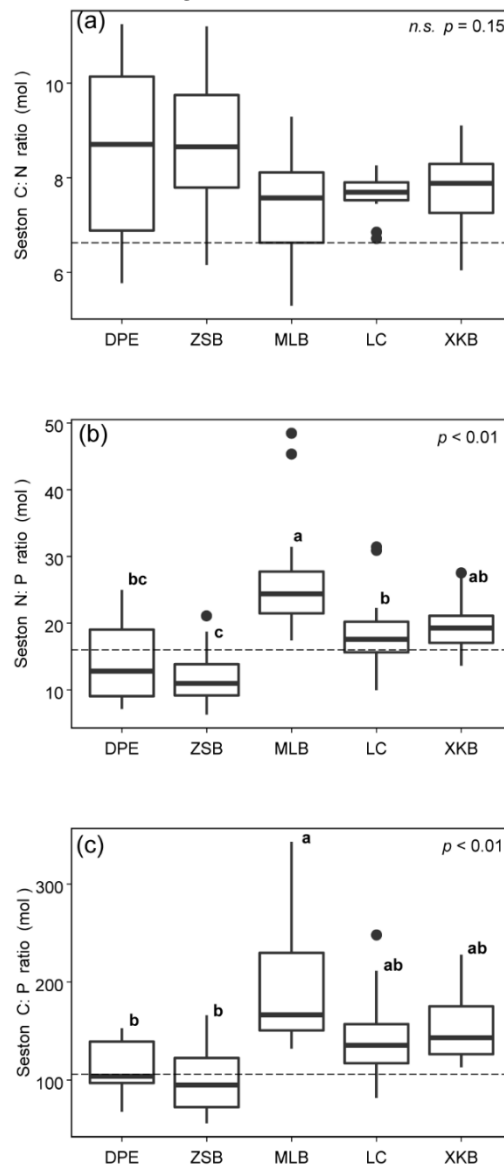


**Figure 2.** Spatial variations in seston stoichiometric ratio of C: N (a), N: P (b) and C: P (c) across different sub-ecotypes across Lake Taihu. Dashed reference lines show classical Redfield ratios. Letters denote significant differences between different location, and *n.s.* indicates no significant differences.

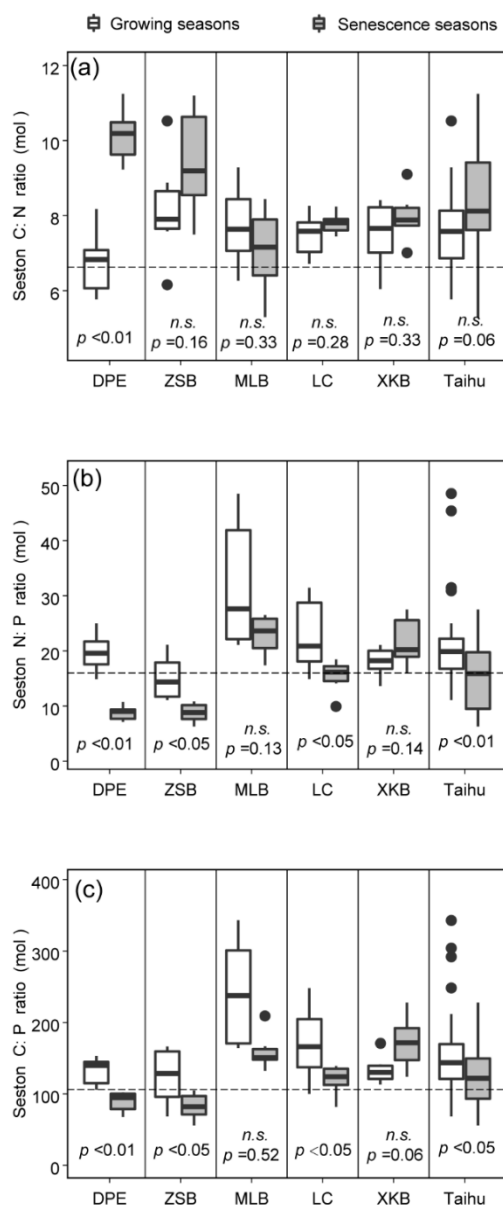


**Figure 3.** Temporal variations in seston stoichiometric ratio of C: N (a), N: P (b) and C: P (c) within different sub-ecotypes across Lake Taihu. Dashed reference lines show classical Redfield ratios. The  $p$  values denote significant differences between different seasons within each site and *n.s.* indicates no significant differences.

### 3.2. PCA of *n*-alkane proxies and source estimation

PCA was conducted to investigate the association of five *n*-alkane proxies and select the most representative proxies. The first three principal components (PCs) could explain 78.9% of the total variance in datasets. Considering the first two components could already explain 71.8% of the total variance, the third components were not shown (Figure 4). PC1 was most positively loaded on ACL (37.2%), followed by CPI1 and TARHC, whereas L/H and Paq scattered in the negative direction and contributed fewer loadings for PC1. Paq was shown as much more positive contribution (68.3%) to PC2 than other proxies which showed lower negative loadings on PC2. For reducing the dependent predictors in following PLSR analysis, ACL and Paq were select to represent the whole datasets. As expected, the new sub dataset was highly correlated to the raw matrix (Mantel test,  $r = 0.82$ ,  $p < 0.01$ ).

ACL serves as a method for identifying terrigenous and aquatic source inputs in sediments, where value higher than 23.3 indicates pronounce contribution from terrestrial seston [35]. Among the seston with high ACL values, seston from submerged and floating macrophytes sources would

have Paq values between 0.48 and 0.94 [26], owing to submerged and floating macrophytes contain abundant mid-chain alkanes (e.g. n-C21, n-C23 and n-C25). Basing on two selected indices, the sources of seston in Lake Taihu could be generally classified into three categories (Figure 5). The first category was characterized as relatively lower ACL values (<23.3), suggesting dominated by algal origins with short-chain *n*-alkanes. The second category was characterized as high ACL values (mean=27.1) and moderate Paq values (0.21-0.47), indicating a major contribution of terrigenous source and minor contribution of macrophytes. The third category was mainly made up of macrophytes detritus (Paq > 0.5) that was from XKB during senescence seasons. Remarkably, similar to stoichiometric ratios, there was also a significant seasonal shift ( $p < 0.05$ ) in seston sources. As shown, most samples in growing seasons were dominated by algal source, and most sestons were dominated by the terrestrial source during senescence seasons. However, this seasonal effect was not shared within all sites. There were no significant changes in sources of seston in XKB and MLB.

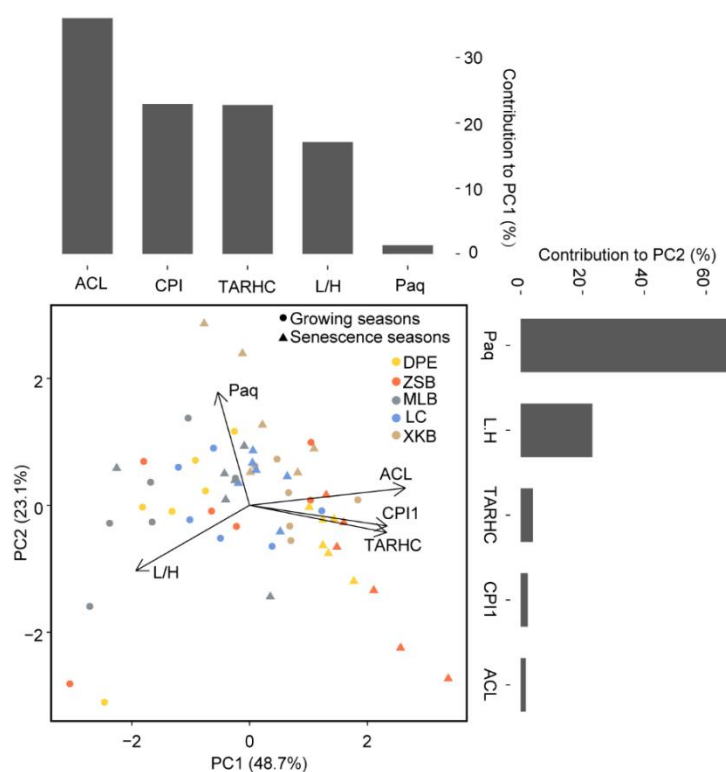


**Figure 4.** PCA plots of *n*-alkanes proxies and their individual contributions to PC1 and PC2.

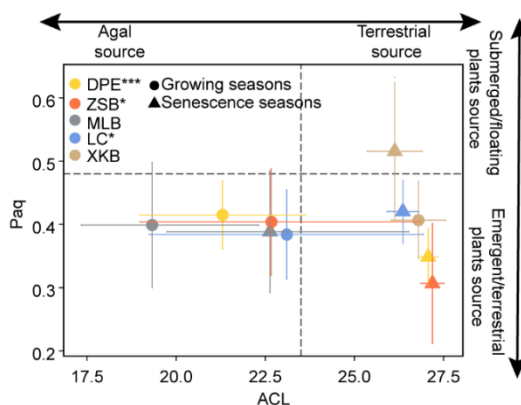


**Figure 5.** Biplot of ACL and Paq distribution across Lake Taihu. Vertical and horizontal reference lines are used for identifying different sources as illustrated. The following \* and \*\*\* symbols denote the significant differences between growing seasons and senescence seasons within each site, with  $p < 0.05$  and  $p < 0.001$ , respectively.

values less than 0.05 and 0.001 respectively. The vertical and horizontal error bars respectively depict  $\pm 1$  standard deviation of Paq and ACL means.

### 3.3. PLSR analysis

Apart from sources indicators, environmental variables (Table S1) in regression models explained around 25% of variations on average (Figure 6a-c). After adding two sources indicators, the explained proportions of PLSR models for N: P and C: P strongly increased from 25.04% to 56.36%, and from 27.65% to 62.41% (Figure 6d-f), respectively. Both ACL and Paq were important predictors according to their VIP scores. Besides, the phosphorus contents were also important in regression models. However, it is noticed that the explanatory ability of PLSR models for C: N was not influenced by additional sources indicators.

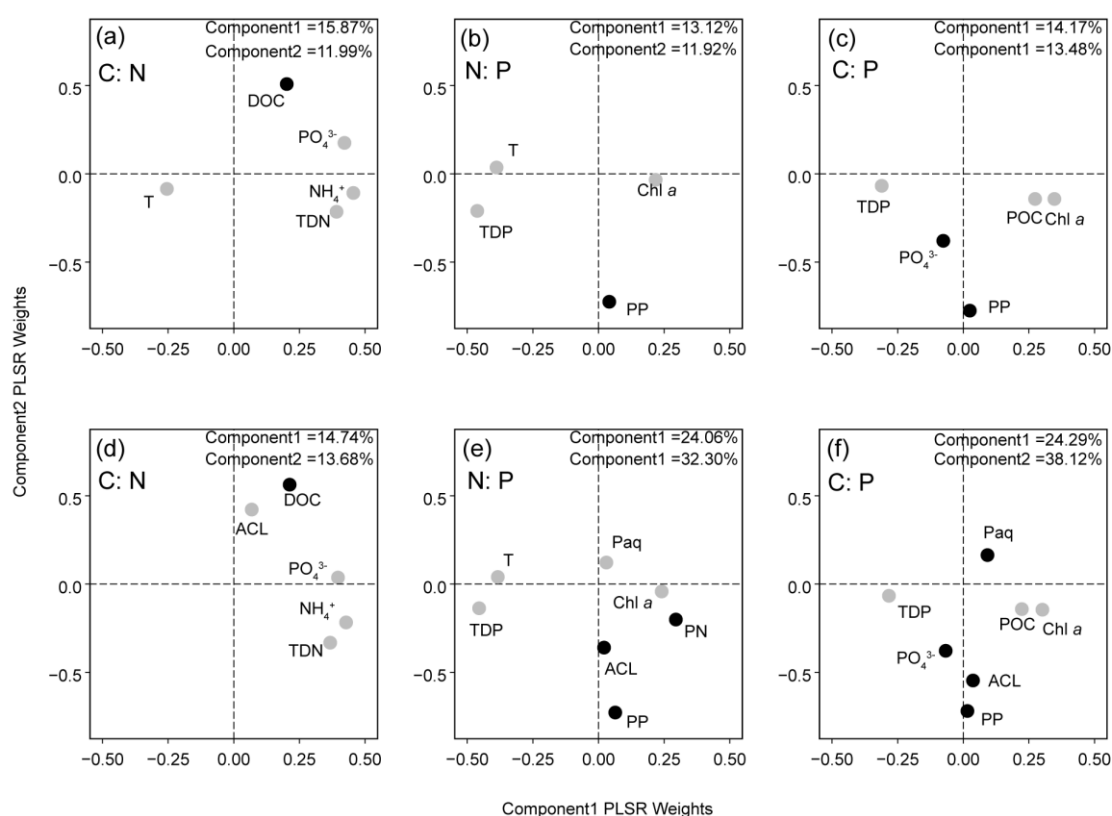


**Figure 6.** Scatterplots of predictors for spatio-temporal variation of seston stoichiometric ratios in Lake Taihu with (d-f) and without source indicators (a-c). Individual predictor weights are directly proportional to the amount of variance explained for each component. The total explained variance of each component are shown in the top right of each plot, and the seston ratios are shown in the top right. VIP of each predictor is indicated as: black solid circles (highly important) and grey solid circles (moderately important). Weakly important predictors are not illustrated in figures.

### 3.4. C: N: P stoichiometric ratios of seston from different sources

As classified above, all samples could be classified into three sources: algal-derived seston (n=23), terrestrial-derived seston (n=33), submerged macrophytes-derived seston (n=4). Statistically, C: N ratios are comparatively consistent between and within seston dominated by different sources (Figure 7a). On the contrary, the average value of N: P (11) and C: P (108) ratios from terrestrial-derived seston significantly lower than those ratios (N: P=23, C: P=183) of algal-derived seston and those ratios (N: P=24, C: P=165) (Figure 7b,c). Accordingly, there were strong negative relationships between ACL and N: P and C: P ratios (Figure 7e,f). Further, within terrestrial-derived seston, these ratios had a significant positive relationship with Paq values (Figure 7h,i).

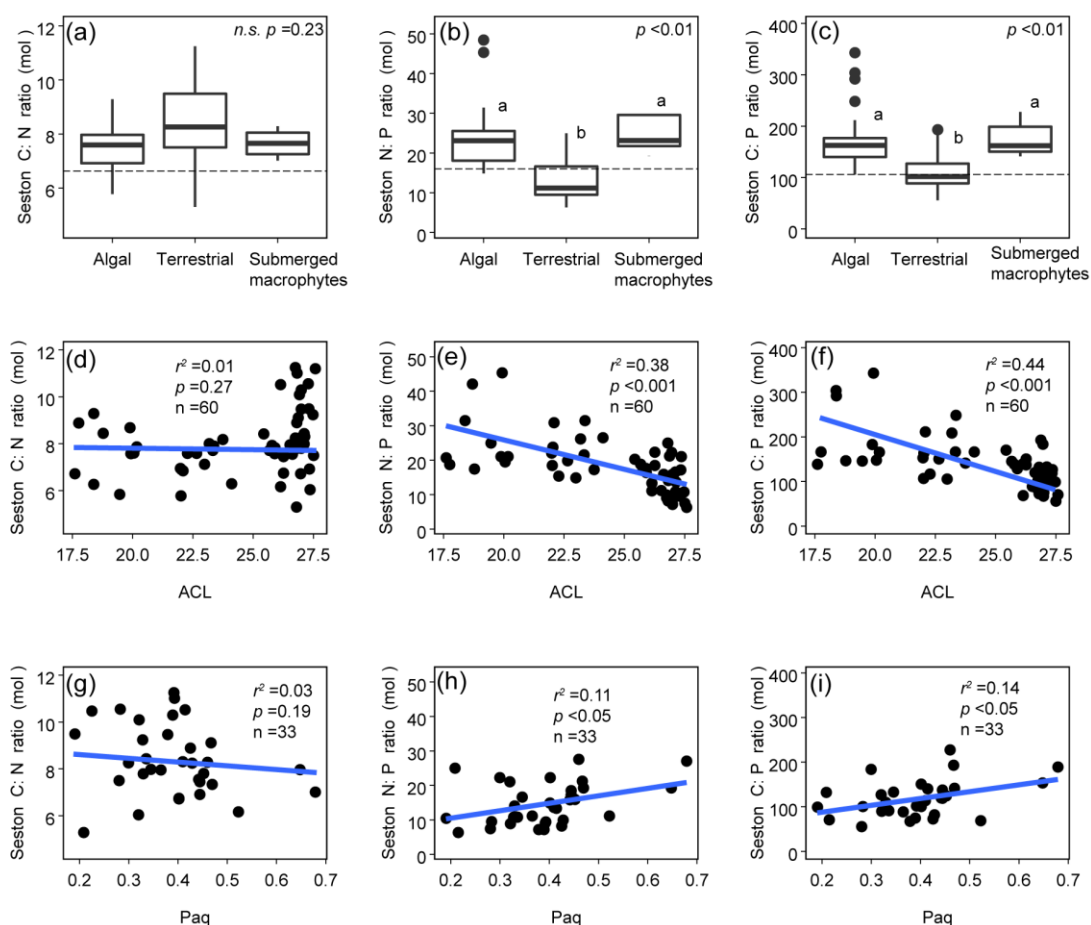


**Figure 7.** Differences and relationships between stoichiometric ratios of seston dominated by different sources. The general differences of each ratio between each source were shown at the top right of corresponding figures in (a-c). Linear relationship between ACL and seston stoichiometric ratios (d-f), and between Paq and stoichiometric ratios of seston dominated by terrestrial sources (g-i).

#### 4. Discussion

As expected for most inland waters, the average value of C: N: P ratio of 143: 19: 1 across Lake Taihu was higher than the classical Redfield ratio (C: N: P = 106: 16: 1) and close to the modified Redfield ratio of 166: 20: 1 as lakes' datasets were integrated in [9]. This ratio was also concomitant with the previous survey [36], which suggested that the seston stoichiometric ratios interannually stable and comparable in Lake Taihu. In general, the seston N: P and C: P ratios varied more widely than C: N ratios, which is a common pattern within freshwater ecosystems [9,13,34]. Basing on the PLSR analysis, two major groups of important predictors were responsible for the flexibility of these two ratios in Lake Taihu: phosphorus and, as we proposed, the indicators of seston sources. Adding ACL and Paq as source indicators considerably increased the predictive power of PLSR models for N: P and C: P ratios, respectively. Additionally, significant negative relationships between ACL and N: P and C: P ratios were observed in this study. These results are statistically supporting our hypothesis that the seston sources are important factors in shaping the spatiotemporal pattern of seston stoichiometric ratios in Lake Taihu and other similar large eutrophic floodplain lakes.

##### 4.1. Highlights of *n*-alkanes proxies rather than elemental ratios as source indicators

The basically consistent C: N ratios around 8 seemed unlikely to support our claim that terrestrial contribution is considerable in Lake Taihu as, typically, C: N ratios of algal origin ranged from 5 to 9 [37]. Depending on this paradigm, the previous study argued that the majority seston was

consistently comprised of algal sources in Lake Taihu, and therefore they mostly explained the strong seasonal changes of seston C: P and N: P ratios from the aspect of algal communities. However, the suitability of C: N as a source indicator is under debate for decades. Its uncertainty has been noted in many works, as it may be confounded by factors such as the incorporation of microbial biomass during biodegradation [38,39] and fixation of inorganic nitrogen on clays [22], both of which could lower the C: N ratio and weaken the divergence between algal and terrestrial origins.

Relatedly, other elemental indicators, such as POC: Chl *a* ratio or stable isotope of  $\delta^{13}\text{C}$ , are not recommended to derive seston sources either. Although POC: Chl *a* ratio is easily obtained and therefore widely used as an alternative indicator to C: N ratio, many studies have announced that its accuracy should be interpreted with caution. POC: Chl *a* ratios of algal biomass could vary over 10-fold (from 35 - 450) over different studies, and depend on properties of the study area, the state of the bloom and the algal species [40,41]. Thus, using a certain ratio of POC: Chl *a* (i.e. 200 or 100) as a threshold to distinguish algal sources and terrestrial sources is not reliable, especially in eutrophic lakes. Similarly, the  $\delta^{13}\text{C}$  signatures of algae vary spatiotemporally, which mainly corresponded with fluctuating inorganic  $\delta^{13}\text{C}$  values in freshwater ecosystems (Meyers, 1997; Meyers and Ishiwatari, 1993).

Compared to elemental indicators, *n*-alkanes proxies are more robust as tools for identifying sources of seston of lakes because they are source-specific and more resistant to biodegradation [30,44–46]. Yet the precise composition of different sources in seston pool could not be fully resolved by *n*-alkanes proxies alone. For example, the contribution of resuspended sediments could not be estimated by lipid biomarkers as they have similar molecular compositions with their primary biogenic sources [46]. Multiple-combined proxies could be a better way in such a complicated ecosystem with high spatiotemporal heterogeneity [46]. Nevertheless, this study supports the utility of using *n*-alkanes proxies to accurately distinguish the sources of seston in eutrophic floodplain lakes.

#### 4.2. Hydrological mixing processes leading to limited spatial heterogeneity

Opposite to our prediction, there are similar temporal patterns between each sub-ecotype. The broad dispersion of algal cells in growing seasons and terrestrial materials in senescence seasons could partly explain the spatial homogeneity. Firstly, most freshwater cyanobacteria contain gas vesicles inside the cells, thus helping cells floating on the surface [51]. These near-surface cells are easily transported by horizontal currents. Secondly, under the south-east Asia monsoon throughout the growing season, horizontal mixing currents accumulate algal biomass in northwest estuary region and, therefore, the terrestrial signals are overridden [24]. For terrestrial materials, given that the shallowness and in Lake Taihu [19], the frequent resuspension leading to the prolonged residence time of these sestons in the water column may be one reason for their horizontal board dispersion. As algal biomass is highly biodegradable and is preferentially utilized by micro-food webs (Shi et al., 2017), the intensive wind-wave disturbance could also provide sufficient dissolved oxygen which accelerates the rapid mineralization of algal-derived seston (Xu et al., 2015). Consequently, more terrestrial materials are preserved in the water column or surficial sediments after algal blooming. These characteristics of Lake Taihu and similar large shallow floodplain lakes will reduce the spatial heterogeneity between distinct sub-ecotypes.

#### 4.3. Seasonal changes in stoichiometric ratios corresponded with seasonal shifts in seston sources

Consistent with other eutrophic lakes, there are significant seasonal changes with lower ratios of N: P and C: P during senescence seasons and higher ratios in the growing seasons [33,34,36]. Apart from the estimation of the source, previous studies used to attribute the pronounced seasonal shifts in seston C: P ratios to a “growth by dilution” hypothesis in eutrophic lakes. That is, while ambient P will initially increase the cellular P-quota, the resulting high algal biomass will eventually end up with limited P quota and assimilating C alone (Hessen et al., 2005). Or some researches explained these shifts by the changes of communities species [36], because diatoms have low cellular C: P ratios than cyanobacteria. However, as illustrated above, these hypotheses only work at a certain

circumstance that seston is consistently dominated by algal origins. Thus, these causes may still work in MLB, where most of seston dominated by algal biomass throughout the study period. Although the differences are not statistically significant, a decreasing trend was observed in this area. But it is clear that there are seasonal shifts from algal-derived seston to terrestrial-derived seston in the estuary and open-water areas, which can represent the majority area of Lake Taihu. That implied the overall seasonal change in stoichiometric ratios may be mainly caused by seasonal shifts in seston sources rather than the seasonal changes in algal cells or communities. On another side, it should be careful to directly speculate the nutrient limitation of algal cells by seston stoichiometric ratios without source information.

Further evidence of role of non-algal sources come from 1) the seston of senescence seasons dominated by terrestrial sources have significant lower N: P and C: P ratios than seston of growing seasons algal origins and 2) significant negative relationships between ACL and N: P and C: P ratios. These indicated that the shift from P-rich terrestrial materials to potentially P-limited algal biomass likely explained the elevated particulate C: P ratios and N: P ratios from senescence seasons to growing seasons. Normally, the terrestrial stoichiometric ratios tend to be higher than the algal biomass due to higher content of structural carbohydrates and lignin [47]. However, the C: P ratios and N: P ratios of terrestrial sources in Lake Taihu were lower on average than those of algal sources but fell within ranges reported for urbanized and agricultural watersheds [48,49]. The similar low ratios were also observed in Lake Erie, where agricultural activities were intensive (They et al., 2017). The low C: P ratios and N: P ratios in seston could result from significant inputs of inorganic P associated with terrestrial seston (i.e. erosional soil) from agriculture-rich catchments surrounding of Lake Taihu [19,50]. 3) significant higher of C: P ratios and N: P ratios of submerged macrophytes-derived seston than terrestrial-derived seston and 4) significant positive relationships between these ratios and Paq among terrestrial seston. These suggest that increasing contribution of submerged macrophyte detritus will elevate the stoichiometric ratios of seston dominated by terrestrial materials because submerged macrophytes mostly have higher ratios than the agricultural soil (Xing et al., 2013). That partly explains the reverse seasonal changes of N: P and C: P ratios in XKB. However, the relative low regression coefficient (~ 0.1) should be noticed, which implies other potential explanatory factors.

#### 4.4. The role of phosphorus in influencing the seston stoichiometric ratios

Alternatively, many studies argued that the dynamics of sestonic phosphorus were largely responsible for systematic changes in C: P and N: P ratios because the seston C and N contents were tightly coupled and C: N ratios varied little [9,12,34,52]. This study agreed with that. PLSR models pointed the phosphorus fractions were important predictors for systematic changes in C: P and N: P ratios across Lake Taihu (Figure 6). Additionally, Pearson correlations also showed significant negative relationships between PP and C: P, N: P ratios (Table S2). However, it should be noticed that the mechanisms behind the dynamics of PP could be different and depending on the source of seston, although the correlations were not source specified. For algal-derived seston, the PP was mostly determined by the dissolved bioavailable phosphorus, especially in nutrient-rich environments [6]. The internal cellular phosphorus could be enriched by high P-uptake in environments with sufficient bioavailable phosphorus and consumed when phosphorus is limited [53]. The significant positive relationship between TDP and PP of algal-derived sestons could support this mechanism here (Figure S1). Interestingly, a similar and stronger positive relationship was shown between TDP and PP of terrestrial-derived sestons (Figure S1). This indicates that there is similar dynamic equilibrium between dissolved and particulate phosphorus in terrestrial materials. The adsorption and desorption of phosphorus on the mineral of terrestrial seston could be one reason for the coupling relationship [54]. Furthermore, the attached microbial communities have the capacity to use the sestonic organic phosphorus as well as inorganic phosphorus, which is partly regulated by the dissolved phosphorus [55]. More accurate data on the different fractions of dissolved and particulate phosphorus would have added further explanatory details.

## 5. Conclusions

To summarise, this study points the priority of accurate estimation of seston source in order to make correct explanation underlining the spatiotemporal patterns in seston C: N: P ratios. Although the similar seasonal patterns could be found in N: P and C: P ratios of Lake Taihu and previous eutrophic lakes. Our results indicate that the seasonal shift here was mainly associated with the shift from terrestrial-derived seston to algal-derived seston rather than the changes in alga taxa or cellular contents. However, owing to the topographic and climate characteristic in Lake Taihu, the seston source and stoichiometric ratios are not site-specific. A greater spatial heterogeneity is expected in other large eutrophic floodplain lakes, where hydrological mixing process is not intensive. Besides, within each source seston, there are distinct mechanisms behind the dynamics of sestonic phosphorus which is also partly responsible for the variations in C: P and N: P ratios. These results highlight, again, that the important role of seston source has been neglected in freshwater ecosystems, which is caused by prior subjective knowledge or applications of insensitive indicators. This study highly recommended the *n*-alkanes proxies rather than C: N ratios or other elemental indicators as source indicators in freshwater ecosystems.

**Acknowledgments:** We thank Jingchen Xue, Yilan Liu and all the staffs from Taihu Laboratory for Lake Ecosystem Research for help with sample collections and analyses. This work is supported by National Natural Science Foundation of China (No. 41571462), the “One-Three-Five” Strategic Planning of Nanjing Institute of Geography and Limnology, CAS (No. NIGLAS2017GH05), and the Key Research Program of Frontier Sciences, CAS (No. QYZDJ-SSW-DQC008).

## References

1. Heuer, H.; Smalla, K. Manure and sulfadiazine synergistically increased bacterial antibiotic resistance in soil over at least two months. *Environ. Microbiol.* **2007**, *9*, 657–666.
2. Demi, L.M.; Benstead, J.P.; Rosemond, A.D.; Maerz, J.C. Experimental N and P additions alter stream macroinvertebrate community composition via taxon-level responses to shifts in detrital resource stoichiometry. *Funct. Ecol.* **2019**, *33*, 855–867.
3. He, H.; Han, Y.; Li, Q.; Jeppesen, E.; Li, K.; Yu, J.; Liu, Z. Crucian carp (*Carassius carassius*) strongly affect C/N/P stoichiometry of suspended particulate matter in shallow warm water eutrophic lakes. *Water* **2019**, *11*.
4. Redfield, A. The biological control of the chemical factors in the environment. *Am. Sci.* **1958**, *46*, 205–221.
5. Koeve, W.; Kähler, P. Balancing ocean nitrogen. *Nat. Geosci.* **2010**, *3*, 383.
6. Martiny, A.C.; Pham, C.T.A.; Primeau, F.W.; Vrugt, J.A.; Moore, J.K.; Levin, S.A.; Lomas, M.W. Strong latitudinal patterns in the elemental ratios of marine plankton and organic matter. *Nat. Geosci.* **2013**, *6*, 279–283.
7. Omta, A.W.; Bruggeman, J.; Kooijman, S.A.L.M.; Dijkstra, H.A. Biological carbon pump revisited: Feedback mechanisms between climate and the Redfield ratio. *Geophys. Res. Lett.* **2006**, *33*, L14613.
8. Frigstad, H.; Andersen, T.; Hessen, D.O.; Naustvoll, L.-J.; Johnsen, T.M.; Bellerby, R.G.J. Seasonal variation in marine C:N:P stoichiometry: can the composition of seston explain stable Redfield ratios? *Biogeosciences* **2011**, *8*, 2917–2933.
9. Sterner, R.W.; Andersen, T.; Elser, J.J.; Hessen, D.O.; Hood, J.M.; McCauley, E.; Urabe, J. Scale-dependent carbon:nitrogen:phosphorus seston stoichiometry in marine and freshwaters. *Limnol. Oceanogr.* **2008**, *53*, 1169–1180.

10. They, N.H.; Amado, A.M.; Cotner, J.B. Redfield Ratios in Inland Waters: Higher Biological Control of C:N:P Ratios in Tropical Semi-arid High Water Residence Time Lakes. *Front. Microbiol.* **2017**, *8*, 1505.
11. Hecky, R.E.; Campbell, P.; Hendzel, L.L. The stoichiometry of carbon, nitrogen, and phosphorus in particulate matter of lakes and oceans. *Limnol. Oceanogr.* **1993**, *38*, 709–724.
12. Hessen, D.O. Determinants of seston C:P-ratio in lakes. *Freshw. Biol.* **2006**, *51*, 1560–1569.
13. Hessen, D.O.; Andersen, T.; Brettum, P.; Faafeng, B.A. Phytoplankton contribution to sestonic mass and elemental ratios in lakes: Implications for zooplankton nutrition. *Limnol. Oceanogr.* **2003**, *48*, 1289–1296.
14. Hessen, D.O.; Van Donk, E.; Gulati, R. Seasonal seston stoichiometry: Effects on zooplankton in cyanobacteria-dominated lakes. *J. Plankton Res.* **2005**, *27*, 449–460.
15. Zhou, Y.; Yao, X.; Zhang, Y.; Zhang, Y.; Shi, K.; Tang, X.; Qin, B.; Podgorski, D.C.; Brookes, J.D.; Jeppesen, E. Response of dissolved organic matter optical properties to net inflow runoff in a large fluvial plain lake and the connecting channels. *Sci. Total Environ.* **2018**, *639*, 876–887.
16. Xu, X.; Li, W.; Fujibayashi, M.; Nomura, M.; Nishimura, O.; Li, X. Predominance of terrestrial organic matter in sediments from a cyanobacteria- blooming hypereutrophic lake. *Ecol. Indic.* **2015**, *50*, 35–43.
17. Wilkinson, G.M.; Pace, M.L.; Cole, J.J. Terrestrial dominance of organic matter in north temperate lakes. *Global Biogeochem. Cycles* **2013**, *27*, 43–51.
18. Zhang, Y.; Jeppesen, E.; Liu, X.; Qin, B.; Shi, K.; Zhou, Y.; Thomaz, S.M.; Deng, J. Global loss of aquatic vegetation in lakes. *Earth-Science Rev.* **2017**, *173*, 259–265.
19. Qin, B.; Xu, P.; Wu, Q.; Luo, L.; Zhang, Y. Environmental issues of Lake Taihu, China. *Hydrobiologia* **2007**, *581*, 3–14.
20. Tang, X.; Krausfeldt, L.E.; Shao, K.; Leclair, G.R.; Stough, J.M.A.; Gao, G.; Boyer, G.L.; Zhang, Y.; Paerl, H.W.; Qin, B.; et al. Seasonal Gene Expression and the Ecophysiological Implications of Toxic *Microcystis aeruginosa* Blooms in Lake Taihu. *Environ. Sci. Technol.* **2018**, *52*, 11049–11059.
21. Zhang, Y.; Yao, X.; Qin, B. A critical review of the development, current hotspots, and future directions of Lake Taihu research from the bibliometrics perspective. *Environ. Sci. Pollut. Res.* **2016**, *23*, 12811–12821.
22. Müller, P.J. C N ratios in Pacific deep-sea sediments: Effect of inorganic ammonium and organic nitrogen compounds sorbed by clays. *Geochim. Cosmochim. Acta* **1977**, *41*, 765–776.
23. Qin, B.; Yang, G.; Ma, J.; Wu, T.; Li, W.; Liu, L.; Deng, J.; Zhou, J. Spatiotemporal Changes of Cyanobacterial Bloom in Large Shallow Eutrophic Lake Taihu, China. *Front. Microbiol.* **2018**, *9*, 451.
24. Cai, J.; Bai, C.; Tang, X.; Dai, J.; Gong, Y.; Hu, Y.; Shao, K.; Zhou, L.; Gao, G. Characterization of bacterial and microbial eukaryotic communities associated with an ephemeral hypoxia event in Taihu Lake, a shallow eutrophic Chinese lake. *Environ. Sci. Pollut. Res.* **2018**, *25*.
25. He, Y.; Zheng, Y.; Pan, A.; Zhao, C.; Sun, Y.; Song, M.; Zheng, Z.; Liu, Z. Biomarker-based reconstructions of Holocene lake-level changes at Lake Gahai on the northeastern Tibetan Plateau. *The Holocene* **2014**, *24*, 405–412.

26. Zhang, Y.; Su, Y.; Liu, Z.; Yu, J.; Jin, M. Lipid biomarker evidence for determining the origin and distribution of organic matter in surface sediments of Lake Taihu, Eastern China. *Ecol. Indic.* **2017**, *77*, 397–408.
27. Poerschmann, J.; Koschorreck, M.; Górecki, T. Organic matter in sediment layers of an acidic mining lake as assessed by lipid analysis. Part II: Neutral lipids. *Sci. Total Environ.* **2017**, *578*, 219–227.
28. Derrien, M.; Yang, L.; Hur, J. Lipid biomarkers and spectroscopic indices for identifying organic matter sources in aquatic environments: A review. *Water Res.* **2017**, *112*, 58–71.
29. Ficken, K.; Li, B.; Swain, D.; Eglinton, G. An n-alkane proxy for the sedimentary input of submerged/floating freshwater aquatic macrophytes. *Org. Geochem.* **2000**, *31*, 745–749.
30. Fang, J.; Wu, F.; Xiong, Y.; Li, F.; Du, X.; An, D.; Wang, L. Source characterization of sedimentary organic matter using molecular and stable carbon isotopic composition of n-alkanes and fatty acids in sediment core from Lake Dianchi, China. *Sci. Total Environ.* **2014**, *473–474*, 410–421.
31. Gao, G.; Zhu, G.; Qin, B.; Chen, J.; Wang, K. Alkaline phosphatase activity and the phosphorus mineralization rate of Lake Taihu. *Sci. China, Ser. D Earth Sci.* **2006**, *49*, 176–185.
32. Taube, R.; Ganzert, L.; Grossart, H.-P.; Gleixner, G.; Premke, K. Organic matter quality structures benthic fatty acid patterns and the abundance of fungi and bacteria in temperate lakes. *Sci. Total Environ.* **2018**, *610–611*, 469–481.
33. Chong, I.G.; Jun, C.H. Performance of some variable selection methods when multicollinearity is present. *Chemom. Intell. Lab. Syst.* **2005**, *78*, 103–112.
34. Prater, C.; Frost, P.C.; Howell, E.T.; Watson, S.B.; Zastepa, A.; King, S.S.E.; Vogt, R.J.; Xenopoulos, M.A. Variation in particulate C : N : P stoichiometry across the Lake Erie watershed from tributaries to its outflow. *Limnol. Oceanogr.* **2017**, *62*, S194–S206.
35. Wang, Z.; Liu, W. Carbon chain length distribution in n-alkyl lipids: A process for evaluating source inputs to Lake Qinghai. *Org. Geochem.* **2012**, *50*, 36–43.
36. Shi, L.; Huang, Y.; Lu, Y.; Chen, F.; Zhang, M.; Yu, Y.; Kong, F. Stocks and dynamics of particulate and dissolved organic matter in a large, shallow eutrophic lake (Taihu, China) with dense cyanobacterial blooms. *J. Oceanol. Limnol.* **2018**, *36*, 738–749.
37. Meyers, P.A.; Ishiwatari, R. Lacustrine organic geochemistry—an overview of indicators of organic matter sources and diagenesis in lake sediments. *Org. Geochem.* **1993**, *20*, 867–900.
38. Guo, W.; Ye, F.; Xu, S.; Jia, G. Seasonal variation in sources and processing of particulate organic carbon in the Pearl River estuary, South China. *Estuar. Coast. Shelf Sci.* **2015**, *167*, 540–548.
39. Tipping, E.; Somerville, C.J.; Luster, J. The C:N:P:S stoichiometry of soil organic matter. *Biogeochemistry* **2016**, *130*, 117–131.
40. Roiha, P.; Westerlund, A.; Nummelin, A.; Stipa, T. Ensemble forecasting of harmful algal blooms in the Baltic Sea. *J. Mar. Syst.* **2010**, *83*, 210–220.
41. Engström-Öst, J.; Koski, M.; Schmidt, K.; Viitasalo, M.; Jónasdóttir, S.; Kokkonen, M.; Repka, S.; Sivonen, K. Effects of toxic cyanobacteria on a plankton assemblage: community development during decay of *Nodularia spumigena*. *Mar. Ecol. Prog. Ser.* **2002**, *232*, 1–14.
42. Hong, C.; Si, Y.; Xing, Y.; Li, Y. Illumina MiSeq sequencing investigation on the contrasting soil bacterial community structures in different iron mining areas. *Environ. Sci. Pollut. Res.* **2015**, *22*, 10788–10799.

43. Meyers, P.A. Organic geochemical proxies of paleoceanographic, paleolimnologic, and paleoclimatic processes. *Org. Geochem.* **1997**, *27*, 213–250.
44. Hesselsoe, M.; Füreder, S.; Schloter, M.; Bodrossy, L.; Iversen, N.; Roslev, P.; Nielsen, P.H.; Wagner, M.; Loy, A. Isotope array analysis of Rhodocyclales uncovers functional redundancy and versatility in an activated sludge. *ISME J.* **2009**, *3*, 1349–1364.
45. Sampei, Y.; Matsumoto, E. C/N ratios in a sediment core from Nakaumi Lagoon, southwest Japan - Usefulness as an organic source indicator -. *Geochem. J.* **2001**, *35*, 189–205.
46. Xu, F.L.; Yang, C.; He, W.; He, Q.S.; Li, Y.L.; Kang, L.; Liu, W.X.; Xiong, Y.Q.; Xing, B. Bias and association of sediment organic matter source apportionment indicators: A case study in a eutrophic Lake Chaohu, China. *Sci. Total Environ.* **2017**, *581–582*, 874–884.
47. Elser, J.J.; Fagan, W.F.; Denno, R.F.; Dobberfuhl, D.R.; Folarin, A.; Huberty, A.; Interlandi, S.; Kilham, S.S.; McCauley, E.; Schulz, K.L.; et al. Nutritional constraints in terrestrial and freshwater food webs. *Nature* **2000**, *408*, 578–580.
48. Veldboom, J.A.; Haro, R.J. Stoichiometric relationship between suspension-feeding caddisfly (Trichoptera: Brachycentridae) and seston. *Hydrobiologia* **2011**, *675*, 129–141.
49. Frost, P.C.; Kinsman, L.E.; Johnston, C.A.; Larson, J.H. Watershed discharge modulates relationships between landscape components and nutrient ratios in stream seston. *Ecology* **2009**, *90*, 1631–1640.
50. Wang, M.; Stokal, M.; Burek, P.; Kroeze, C.; Ma, L.; Janssen, A.B.G. Excess nutrient loads to Lake Taihu: Opportunities for nutrient reduction. *Sci. Total Environ.* **2019**, *664*, 865–873.
51. Wu, X.; Kong, F.; Chen, Y.; Qian, X.; Zhang, L.; Yu, Y.; Zhang, M.; Xing, P. Horizontal distribution and transport processes of bloom-forming *Microcystis* in a large shallow lake (Taihu, China). *Limnologica* **2010**, *40*, 8–15.
52. Frigstad, H.; Andersen, T.; Hessen, D.O.; Naustvoll, L.; Johnsen, T.M.; J Bellerby, R.G. Seasonal variation in marine C:N:P stoichiometry: can the composition of seston explain stable Redfield ratios? *Biogeosciences* **2011**, *8*, 2917–2933.
53. Hessen, D.O.; van Donk, E.; Gulati, R. Seasonal seston stoichiometry: effects on zooplankton in cyanobacteria-dominated lakes. *J. Plankton Res.* **2005**, *27*, 449–460.
54. Tang, H.; Zhao, H.; Li, Z.; Yuan, S.; Li, Q.; Ji, F.; Xiao, Y. Phosphorus sorption to suspended sediment in freshwater. *Proc. Inst. Civ. Eng. Water Manag.* **2017**, *170*, 231–242.
55. Güsewell, S.; Gessner, M.O. N:P ratios influence litter decomposition and colonization by fungi and bacteria in microcosms. *Funct. Ecol.* **2009**, *23*, 211–219.